

Bacterial Magnetosomes as Novel Platform for the Presentation of Immunostimulatory, Membrane-Bound Ligands in Cellular Biotechnology

Frank Mickoleit, Valérie Jérôme, Ruth Freitag,* and Dirk Schüler*

Cell–cell interactions involving specific membrane proteins are critical triggers in cellular development. Ex vivo strategies to mimic these effects currently use soluble proteins or (recombinant) presenter cells, albeit with mixed results. A promising alternative are bacterial magnetosomes, which can be selectively transformed into cell-free membrane–protein presenters by genetic engineering. In this study, the human CD40 Ligand (CD40L), a key ligand for B cell activation, is expressed on the particle surface. Functionality is demonstrated on sensor cells expressing the human CD40 receptor. Binding of CD40L magnetosomes to these cells triggers a signaling cascade leading to the secretion of embryonic alkaline phosphatase. Concomitantly, the CD40–CD40L interaction is strong enough to allow cell recovery by magnetic sorting. Overall, this study demonstrates the potential of magnetosomes as promising cell-free tools for cellular biotechnology, based on the display of membrane-bound target molecules, thereby creating a biomimetic interaction.

Biological reactions triggered by the interaction of specific membrane-bound ligands (L) with cellular receptors are of high interest in tissue engineering, but also for directed stem cell differentiation or in cancer immunotherapy.^[1,2] Current approaches to mimic such reactions ex vivo use soluble multimers of the ligand or present the ligand on the surface of (genetically modified) mammalian cells. Both approaches are known to have disadvantages: soluble multimers are often not nearly as active as their natural membrane-anchored counterparts, while ligand


presenting (recombinant) cells require complex co-cultivation conditions and threaten to contaminate the target cell population. A pertinent example for a specific cell activation via a membrane-bound ligand is the proliferation and differentiation of (antibody producing) B cells by interaction of the CD40 receptor with its physiological ligand, namely CD40L.^[3] For a successful stimulation of B cells, both the presentation of CD40L as transmembrane protein and the in situ oligomerization into a trimer is assumed to be crucial.^[1,4,5] Successful ex vivo expansion of B cells has been achieved using irradiated peripheral blood mononuclear cells (PBMCs) or recombinant cells acting as feeder and CD40L presenting cells.^[4,6] However, the recombinant cells are not openly accessible and, most importantly, contamination with xenogeneic components

limit their use for clinical applications. Therefore, a substitute presentation system with reduced drawbacks and efficacy comparable to the natural membrane-bound CD40L is highly desirable.

Such a solution may be provided by bacterial magnetosomes, biogenic nanoparticles produced by magnetotactic bacteria. In the alphaproteobacterium *Magnetospirillum gryphiswaldense* they consist of a monocrystalline magnetite core enveloped by a lipid membrane, which contains a set of magnetosome-specific proteins.^[7,8] The particles exhibit unprecedented characteristics like strong magnetization, as well as uniform shape and size, which makes them highly attractive for biomedical and biotechnological applications. Furthermore, magnetosomes can be genetically engineered by expression of foreign proteins as fusions to highly abundant magnetosome membrane (Mam) proteins. Using this approach, the feasibility to express antibodies, fluorophores, enzymes and receptors was already demonstrated.^[9,10] In addition to stable protein display, it can be assumed that the oligomerization of monomeric subunits into functional multimeric structures is facilitated, as recently has been shown for enzymes like the glucuronidase GusA or glucose oxidase.^[11,12] The presentation of a functional multimeric ligand, such as CD40L, to trigger a receptor response is significantly more challenging because steric hindrances linked to the size of the interaction partners conceivably present a bottleneck. However, prompted by the current state-of-the-art we hypothesized that a trans-presentation of CD40L on magnetosomes might allow a successful trimerisation required for biological activity, thereby mimicking the natural membrane-bound state of the

Dr. F. Mickoleit, Prof. D. Schüler
Department Microbiology
University of Bayreuth
Universitätsstraße 30
D-95447 Bayreuth, Germany
E-mail: dirk.schueler@uni-bayreuth.de

Dr. V. Jérôme, Prof. R. Freitag
Department Process Biotechnology
University of Bayreuth
Universitätsstraße 30
D-95447 Bayreuth, Germany
E-mail: ruth.freitag@uni-bayreuth.de

 The ORCID identification number(s) for the author(s) of this article can be found under <https://doi.org/10.1002/adbi.201900231>.

© 2020 The Authors. Published by WILEY-VCH Verlag GmbH & Co. KGaA, Weinheim. This is an open access article under the terms of the Creative Commons Attribution License, which permits use, distribution and reproduction in any medium, provided the original work is properly cited.

DOI: 10.1002/adbi.201900231

ligand. Magnetosomes allow for a feeder-free culture system, thereby reducing common risk in biotechnological products derived from cell lines such as contamination with pathogenic agents and/or persistence of glycoprotein molecules (shown for murine presenting feeder cells), which could result in severe immune reactions against any transplanted cell product.^[13]

To study effects of ligand density, three variants of CD40L displaying magnetosomes were generated using two Mam proteins with different abundances, namely MamC and MamG (60 or 165 copies per particle, respectively),^[12,14] as anchors. A 702 bp construct encoding a flexible 17 amino acid linker coupled to the extracellular codon-optimized CD40L domain (amino acids 51–261)^[15] was fused either to the *mamC* or *mamG* sequence, and set under the control of a transcriptional unit optimized for constitutive high-level magnetosome expression (Figure S1, Supporting Information).^[16] *mamC-cd40l* or *mamG-cd40l* cassettes were transferred to the wildtype (WT) of *M. gryphiswaldense*, thereby generating strains C-CD40L and G-CD40L (Figure 1). As the WT still harbors native, unfused gene copies of *mamG* or *mamC* in equal amounts, it can be assumed that approximately 30 (G-CD40L, calculated M_w : 35.3 kDa) or 83 CD40L copies (C-CD40L, calculated M_w : 37.9 kDa) were displayed on the surfaces of the respective particles. In addition, the *mamC-cd40l* expression cassette was inserted into the isogenic Δ *mamC* strain (which lacks the corresponding wildtype allele). The resulting strain, Δ C-CD40L, was expected to display up to 165 copies of CD40L on the magnetosome membrane.

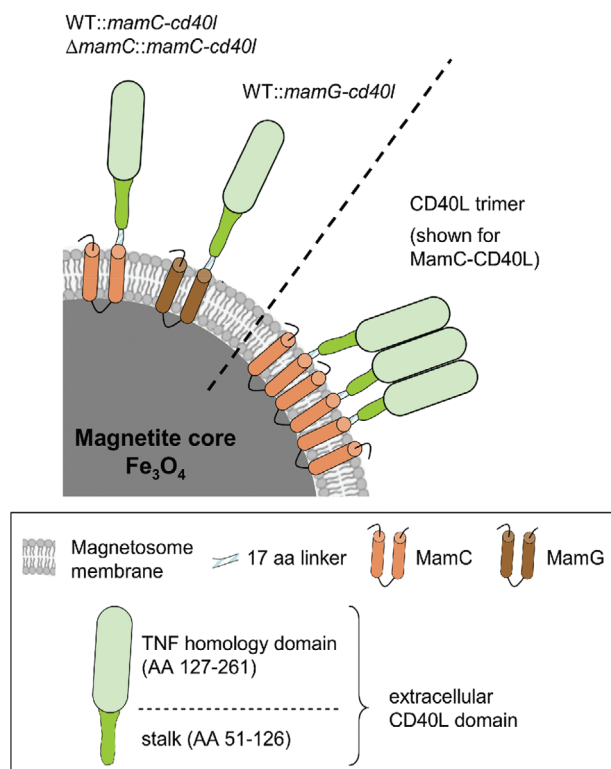


Figure 1. Magnetosome display of CD40L moieties (expressed as hybrid-proteins on the particle surface), and formation of biologically active, trimeric structures (shown for MamC-CD40L). Size of particle and proteins not to scale.

Phenotypically, strains C-CD40L, Δ C-CD40L, and G-CD40L were undistinguishable from each other and from the WT (Figure 2). All strains biomineralized up to 70 magnetosomes per cell arranged in a chain-like manner. transmission electron microscopy (TEM) analysis of isolated CD40L-decorated magnetosomes showed WT-like size distributions (Figure S2, Supporting Information) and particle diameters ($40 < r_h < 55$ nm; Table S1, Supporting Information), with the magnetite cores being surrounded by an electron-light organic shell (3–5 nm) representing the (CD40L-functionalized) magnetosome membrane.

CD40L display on the magnetosome surface was verified by denaturing sodium dodecyl sulfate polyacrylamide gel electrophoresis (SDS-PAGE) with subsequent Western blotting using polyclonal antibodies against the CD40L extracellular domain. Protein bands in the expected molecular mass range were detected for the magnetosome membrane fractions of all three recombinant strains (Figure 3A). In case of C-CD40L and Δ C-CD40L additional bands were visible at 15 or 25 kDa, respectively, corresponding to the tumor necrosis factor homology domain or monomeric CD40L (cleaved off the membrane anchor). As the magnetosome membrane fractions were prepared under “mildly” denaturing conditions, it is furthermore tempting to assume that the additional bands of 81 kDa (for Δ C-CD40L) and 118 kDa (for C-CD40L) might represent dimeric or trimeric hybrid-CD40L (calculated theoretical mass 114 kDa or 76 kDa, respectively), which would furthermore indicate the successful oligomerization of the ligand. No bands were detected in the membrane preparation from WT magnetosomes, whereas for the commercial soluble recombinant human CD40L (rhCD40L) reference a band of about 15 kDa was visible, corresponding to the predicted molecular mass of monomeric rhCD40L (16.3 kDa).

For testing biological activity, magnetosome “concentrations” of approximately $50 \mu\text{g Fe mL}^{-1}$ (corresponding to 2.8×10^{11} particles per mL) were desired. The colloidal stability of such suspensions was estimated by dynamic light scattering (DLS). Hydrodynamic diameters of the CD40L magnetosome variants in storage buffer (10 mM 4-(2-hydroxyethyl)-1-piperazineethanesulfonic acid (HEPES), pH 7.0) were all in the range as determined by TEM and similar to non-functionalized WT magnetosomes (Table S1, Supporting Information), thereby confirming colloidal stability. In addition, the stability of all CD40L-functionalized magnetosomes in cell culture medium (Dulbecco’s modified eagle’s medium-10% fetal calf serum, up to 40 h incubation) was verified to exclude effects caused by non-specific interactions with media compounds (Figure S3, Supporting Information). For non-decorated WT magnetosomes, the hydrodynamic diameter increased two-fold during incubation indicating the formation of small agglomerates or particle chains. A similar trend, though less pronounced, was observed for G-CD40L. In case of C-CD40L and Δ C-CD40L even a prolonged incubation in cell culture medium did not have a significant effect on the particle size. This may be due to electrostatic repulsion/steric hindrance caused by the high number of presented ligands. CD40L magnetosomes can thus be used for cell culture applications at least at final concentrations $\leq 50 \mu\text{g Fe mL}^{-1}$.

The biological activity of the CD40L-functionalized magnetosomes was first tested using recombinant human embryonic kidney (HEK)-CD40L sensor cells, which express the human

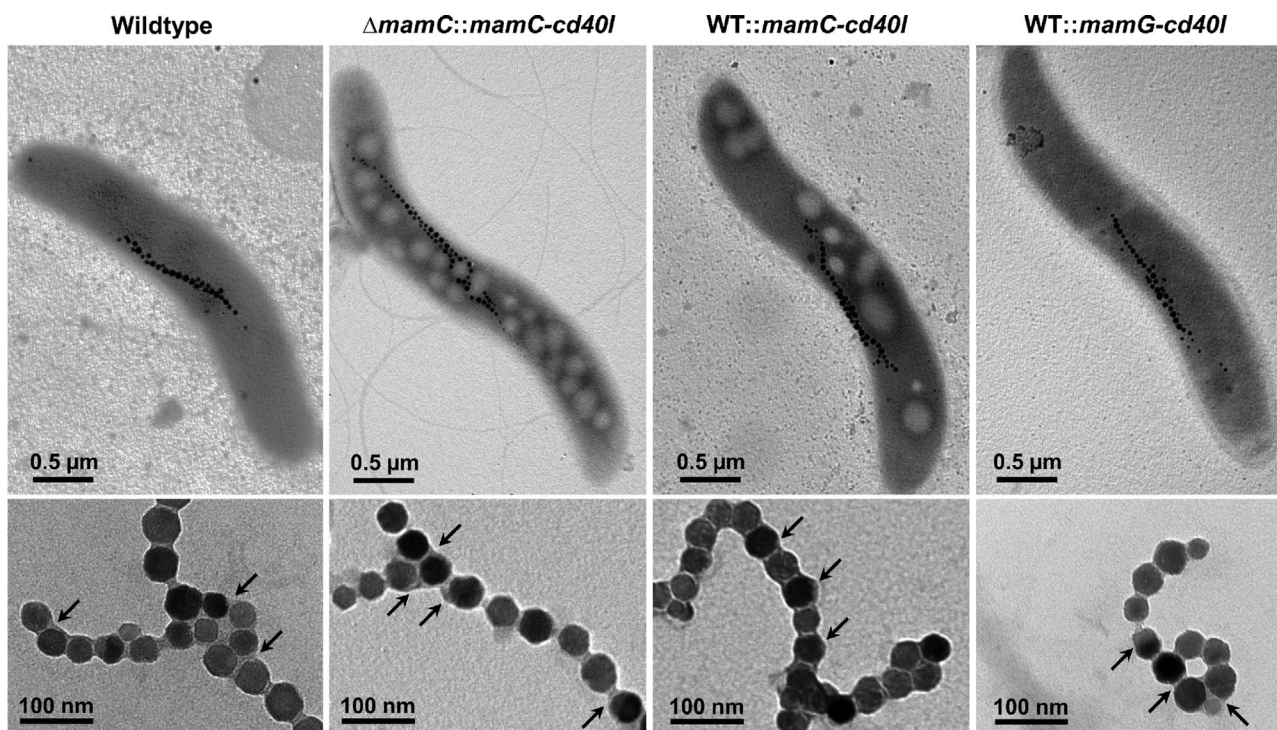


Figure 2. Upper panel: TEM micrographs of the *M. gryphiswaldense* WT and *cd40l* expressing strains. Lower panel: TEM micrographs of isolated (CD40L-functionalized) magnetosomes. The surrounding magnetosome membrane is indicated by arrows.

CD40 (hCD40) receptor on their surfaces together with an NF- κ B-inducible SEAP (human secreted embryonic alkaline phosphatase). Interaction of the CD40 receptor with CD40L leads to the activation-correlated secretion of SEAP into the cell culture supernatant. SEAP was quantified in the cell culture supernatant using a novel assay recently described.^[17] We first verified that the necessary addition of up to 20% (v/v) of a hypotonic 25 mM

HEPES buffer did not significantly affect the viability of the cells (Table S2, Supporting Information). Subsequently, the sensor cells (16×10^4 cells mL⁻¹) were incubated with 50 μ L (corresponding to 50 μ g Fe mL⁻¹ or 10^7 – 10^8 ligand molecules per cell) of the respective CD40L-magnetosome suspensions. As controls, we tested magnetosomes “decorated” with protein arrays of similar molecular mass as CD40L (PS magnetosomes,^[18] displaying

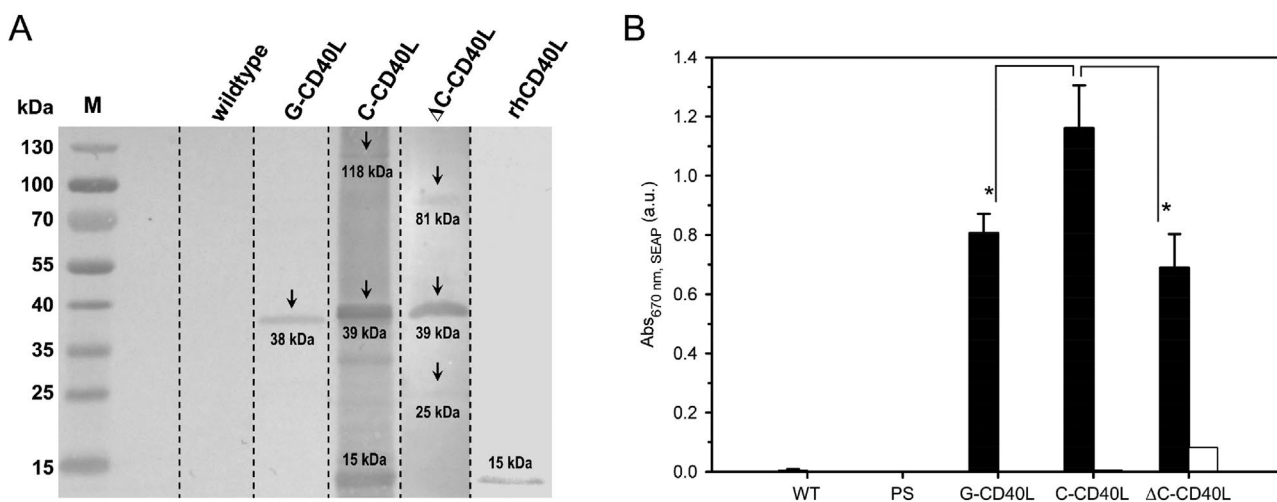


Figure 3. A) Qualitative analysis of CD40L display on the magnetosome surface using SDS-PAGE with subsequent Western blotting (immunochemical detection). Sample volumes correspond to 32 μ g Fe per lane. WT magnetosomes and recombinant, soluble rhCD40L (2 μ g) were used as controls. B) Stimulatory effects of CD40L-functionalized magnetosomes on HEK-CD40L sensor cells. WT ($n = 3$), PS ($n = 3$), G-CD40L ($n = 3$), Δ C-CD40L ($n = 3$), and C-CD40L ($n = 2$) magnetosomes as well as the corresponding particle-free supernatants ($n = 2$) were tested for their ability to stimulate HEK-CD40L cells (16×10^4 cells mL⁻¹). Black bars: magnetosome suspensions, white bars: corresponding supernatants. Statistically significant differences ($p < 0.05$) are denoted by *.

arrays of 85 polyserine residues fused to MamC) and WT magnetosomes to confirm the specificity of the response. Cells were also incubated with 50 μL of the centrifuged magnetosome supernatants to exclude the presence of soluble, non-membrane bound CD40L released from the magnetosome membrane in the added suspension, Figure 3B.

As expected, neither WT nor PS magnetosomes induced SEAP production. In case of the magnetosome supernatants, only background activities were measured, indicating that CD40L stayed stably immobilized on the magnetosome surface. By contrast, all CD40L-functionalized magnetosomes elicited a strong response reminiscent of cell–cell activation in the sensor cells. The effect of G-CD40L and ΔC -CD40L on the cells was similar, despite considerable differences in ligand density. Up to 1.6-fold more SEAP was produced when the cells were in contact with C-CD40L magnetosomes, suggesting that an optimum ligand density exists, which induces the highest response. Based on the frequency of the respective Mam proteins, G-CD40L magnetosomes (about 30 ligands per particle) would theoretically allow the formation of 10 CD40L trimers. C-CD40L magnetosomes (83 monomers) could display up to 27 trimers, while for ΔC -CD40L magnetosomes (165 CD40L monomers) a theoretical number of 55 trimers is calculated. The biological activity of CD40L strongly depends on the formation of these (multi)trimers.^[19,20] Higher ligand densities might impede CD40L trimerization via steric hindrances on an “overcrowded” surface. As mentioned above, the mean diameters of the magnetosomes and their size distributions were rather similar for the three CD40L-functionalized magnetosomes. Therefore, we can exclude magnetosome size effects.

As specifically interacting magnetic nanoparticles, magnetosomes are also putative capturing agents. To date they have mostly been used to capture soluble analytes.^[9,21,22] However, as trimeric CD40L can be expected to bind CD40 with high apparent affinity in the low nM range,^[23] we tested the possibility of capturing entire cells using CD40L magnetosomes. Sensor cells were incubated with 50 μL of a CD40L-magnetosome suspension (25 and 50 $\mu\text{g Fe mL}^{-1}$ in binding buffer) and subsequently subjected to cell sorting using magnetic racks. WT and PS magnetosomes as well as just 10 mM HEPES buffer were used as negative controls. Although full recovery rates of the HEK-CD40L cells could not be achieved (and additional improvements of the experimental setting might be required), the incubation with CD40L magnetosomes allowed to retain almost 50% of the cells in the magnetic field (Table 1). Interestingly, neither the ligand density nor the magnetosome concentration seemed to play a crucial role in cell recovery. These results show that the interaction between the immobilized CD40L and its receptor is strong enough to allow for cell sorting. When incubated with HEPES or WT/PS magnetosomes, less than 20% of the HEK-CD40L cells were retained.

In conclusion, we show that hCD40L functionalized magnetosomes can effectively bind to the corresponding cellular receptor and elicit biological responses, as demonstrated here by using SEAP secreting sensor cells as model. This proves that the presentation of a ligand as a membrane-anchored protein on the surface of magnetosomes can indeed function as a surrogate for recombinant (genetically engineered) cells, which are the current gold standard. Our results also underline the

Table 1. Magnetic sorting of HEK-CD40L cells using functionalized magnetosomes.

	Cell recovery [%]	
	50 $\mu\text{g Fe mL}^{-1}$ magnetosomes	25 $\mu\text{g Fe mL}^{-1}$ magnetosomes
10 mM HEPES	13.4 \pm 1.3	9.8 \pm 3.5
WT	15.1 \pm 4.2	n.d.
PS	19.0 \pm 2.9	n.d.
G-CD40L	40.1 \pm 5.2	47.5 \pm 4.7
C-CD40L	48.7 \pm 4.4	42.2 \pm 8.6
ΔC -CD40L	42.3 \pm 1.6	47.7 \pm 7.3

Data correspond to cells present in the magnetically retained fraction as percentage of the total cell number during incubation. n.d.: not determined. Data represent mean values \pm SD for $n = 2$ (50 $\mu\text{g Fe mL}^{-1}$ magnetosomes) and $n \geq 3$ (25 $\mu\text{g Fe mL}^{-1}$ magnetosomes).

potential of (ligand) functionalized magnetosomes for targeted magnetic cell-sorting. Since several magnetosome membrane anchors could be simultaneously utilized,^[12] the density of displayed functional groups might be further adjusted over a certain range. Hence, the magnetosome display system provides a versatile all-in-one tool, which not only allows a highly selective, cell-free membrane-bound presentation, but also a ligand-prompted magnetic cell sorting.

Experimental Section

Detailed information about experimental procedures is available as Supporting Information.

Supporting Information

Supporting Information is available from the Wiley Online Library or from the author.

Acknowledgements

F.M. and V.J. contributed equally to this work. Julian Schub is acknowledged for contributing some of the data produced as part of his Master thesis. The authors thank Matthias Schlotter (Dept. Microbiology) for expert technical assistance. This work was supported by the Deutsche Forschungsgemeinschaft (DFG), grant 411774929 to R.F. and grant Schu1080/9-2 to D.S., and the European Research Council (ERC) under the European Union’s Horizon 2020 research and innovation programme, grant agreement No 692637 to D.S..

Conflict of Interest

The authors declare no conflict of interest.

Keywords

bacterial magnetosomes, CD40, membrane proteins, nanoparticles, receptor-ligand interaction

Received: September 23, 2019
Revised: January 16, 2020
Published online: February 7, 2020

- [1] R. S. Kornbluth, M. Stempniak, G. W. Stone, *Int. Rev. Immunol.* **2012**, *31*, 279.
- [2] A. Wyzgol, N. Muller, A. Fick, S. Munkel, G. U. Grigoleit, K. Pfizenmaier, H. Wajant, *J. Immunol.* **2009**, *183*, 1851.
- [3] C. van Kooten, J. Banchereau, *J. Leukocyte Biol.* **2000**, *67*, 2.
- [4] J. Banchereau, F. Bazan, D. Blanchard, F. Brière, J. P. Galizzi, C. v. Kooten, Y. J. Liu, F. Rousset, S. Saeland, *Annu. Rev. Immunol.* **1994**, *12*, 881.
- [5] K. Wennhold, A. Shimabukuro-Vornhagen, M. von Bergwelt-Baildon, *Transfus. Med. Hemoth.* **2019**, *46*, 36.
- [6] D. Pinna, D. Corti, D. Jarrossay, F. Sallusto, A. Lanzavecchia, *Eur. J. Immunol.* **2009**, *39*, 1260.
- [7] C. Jogler, D. Schüler, *Annu. Rev. Microbiol.* **2009**, *63*, 501.
- [8] R. Uebe, D. Schüler, *Nat. Rev. Microbiol.* **2016**, *14*, 621.
- [9] G. Vargas, J. Cypriano, T. Correa, P. Leão, D. Bazyliński, F. Abreu, *Molecules* **2018**, *23*, 2438.
- [10] F. Mickoleit, D. Schüler, *Bioinspir. Biomim. Nan.* **2019**, *8*, 86.
- [11] F. Mickoleit, D. Schüler, *Adv. Biosyst.* **2018**, *2*, 1700109.
- [12] F. Mickoleit, C. Lanzloth, D. Schüler, **2019**, unpublished.
- [13] G. N. Stacey, F. Cobo, A. Nieto, P. Talavera, L. Healy, A. Concha, *J. Biotechnol.* **2006**, *125*, 583.
- [14] O. Raschdorf, F. Bonn, N. Zeytuni, R. Zarivach, D. Becher, D. Schüler, *J. Proteomics* **2018**, *172*, 89.
- [15] M. Naito, U. Hainz, U. E. Burkhardt, B. Fu, D. Aho, K. E. Stevenson, M. Rajasagi, B. Zhu, A. Alonso, E. Witten, K. Matsuoka, D. Neuberger, J. S. Duke-Cohan, C. J. Wu, G. J. Freeman, *Cancer Immunol. Immunother.* **2013**, *62*, 347.
- [16] S. Borg, J. Hofmann, A. Pollithy, C. Lang, D. Schüler, *Appl. Environ. Microbiol.* **2014**, *80*, 2609.
- [17] V. Jérôme, R. Freitag, D. Schüler, F. Mickoleit, *Anal. Biochem.* **2019**, *585*, 113402.
- [18] F. Mickoleit, D. Schüler, presented at the Annual Conf. of the Association for General and Applied Microbiology, Jena, Germany, March **2016**.
- [19] X.-h. He, L.-h. Xu, Y. Liu, *Acta Pharmacol. Sin.* **2006**, *27*, 333.
- [20] G. J. Mazzei, M. D. Edgerton, C. Losberger, S. Lecoanet-Henchoz, P. Graber, A. Durandy, J.-F. Gauchat, A. Bernard, B. Allet, J.-Y. Bonnefoy, *J. Biol. Chem.* **1995**, *270*, 7025.
- [21] C. Sun, J. S. H. Lee, M. Zhang, *Adv. Drug Delivery Rev.* **2008**, *60*, 1252.
- [22] A. Pollithy, T. Romer, C. Lang, F. D. Müller, J. Helma, H. Leonhardt, U. Rothbauer, D. Schüler, *Appl. Environ. Microbiol.* **2011**, *77*, 6165.
- [23] L. Ganesan, E. Margolles-Clark, Y. Song, P. Buchwald, *Biochem. Pharmacol.* **2011**, *81*, 810.